Int. J. Solids Structures, 1969, Vol. 5, pp. 175 to 190. Pergamon Press. Printed in Great Britain

A QUASI-STATIC THERMOELASTIC ANALYSIS OF A PROPAGATING CRACK

ROBERT A. LUCAS

Department of Mechanical Engineering, Lehigh University, Bethlehem, Pennsylvania

Abstract—The effects of heat generation by the plastic deformations occurring at the tip of a running crack in quasi-brittle materials is considered. The changes in the surrounding elastic stress field are examined for the case of a semi-infinite, constant velocity crack. It is found that the stresses immediately preceding the propagating crack are reduced in intensity as a natural consequence of a material's irreversibility and that the magnitude of this reduction increases with increasing crack velocity.

NOTATION

C	specific heat
E, ν, λ, μ	elastic constants
J	mechanical equivalent of heat
K, K^*	stress intensity factors
K'	coefficient of heat conduction
$k =$	$(n+1)\pi/\beta$
$k^* =$	$(3\lambda+2\mu)\alpha$
p	Mellin parameter
q_0	strength of the heat source
R	radius of the region of heat input
r, θ, z, t	space and time coordinates
r', θ'	location of heat source
s	Laplace parameter
T	temperature
$t^* =$	$R^2/4\kappa$
$\bar{t} =$	r/V
u, v	r, θ-components of displacement vector
U_p	plastic work
V	crack velocity
α	coefficient of thermal expansion
β	half-wedge angle
κ	thermal diffusivity
ρ	density

INTRODUCTION

In the study of material behavior it is found that for any real solid a limiting velocity of fracture propagation exists. For the past two decades investigators have measured and analytically estimated the level of this limiting fracture velocity. Explanations have been offered based on static, quasi-static, and dynamic considerations. However, because of the complexity of the phenomena both experimental results and analytical evaluations still leave much unexplained. This is particularly true for the quasi-brittle materials and the complicating effects of environmental temperature.

A comprehensive summary of the current crack propagation theories can be found in [1] by F. Erdogan. Briefly, the results indicate that by a dynamic analysis of a sufficiently large body, in which the resistance to fracture is constant and the fracture surface is restricted to a plane, the fracture velocity of the solid would approach the Rayleigh surface wave velocity. Analytical results also show that at fracture velocities above 0·6 to 0·7 of the elastic-shear-wave velocity, c_2, the plane of the crack no longer is the maximum cleavage plane. Hence, straight crack propagation in an isotropic solid is an unstable process and either a slight material imperfection or a superimposed nonsymmetric secondary stress component would cause the crack to bifurcate.

On the other hand, experimental investigations show that under normal conditions the terminal fracture velocity in a solid may be as low as 0·2 c_2 to 0·5 c_2. It is also found, in spite of the known embrittling effects which occur at high strain rates in elasto-plastic and viscoelastic materials, that greater fracture resistance results at the higher fracture velocities. In general it is agreed that the reason for such low velocities is the dependence of the fracture energy, which is the material parameter characterizing the fracture resistance of the solid, on the fracture velocity. The fracture energy has two main components; the conventional surface energy of the solid, and the dissipative energy caused by the irreversible phenomena occurring in the dissipation zone around the periphery of the propagating crack. In most technological materials the surface energy is very small compared to dissipation and is likely to be independent of the crack velocity. Again in real materials, the main source of irreversibility is the plastic deformations and/or the viscous flow.

For some time it has been noted that at the slip bonds the local plastic work may cause relatively high temperature gradients. As early as 1944 Zener and Hollomon [2] reported that in their high strain rate tests local metallurgical changes occurred which are characteristic of steel being rapidly quenched from a high state of temperature. Similar concepts were also used by Nadai [3] to explain Wessel's experimental results of ductile metals at extremely low test temperatures. Recently, in metallurgical examinations of fracture surfaces, Sullivan [4] has found evidence of localized material quenching.

In the evaluation of the deformations of solids, considered on a bulk basis, it has been reasoned that even if the entire plastic work is transformed into heat, the resulting temperature rise of the solid would at most be a few degrees Fahrenheit. This and the relatively high diffusion rates of most materials at the typical deformation speeds considered, have been sufficiently valid reasons for investigators to ignore any thermal effects in their studies. However, in the case of quasi-brittle fracture propagation these same effects are no longer bulk occurrences. Rather, they are highly localized and correspondingly magnified phenomena.

For example, consider the heat generation and the resulting thermoelastic coupling caused by the plastic or viscous deformations occurring at the tip of an advancing crack. In this case these effects are occurring in the region that has the greatest influence on the propagation behavior of the crack. The density of the plastic work causing heat generation, being proportional to the local plastic strains, may also be considerably high when local material failure occurs at the crack front. Furthermore, the diffusion of the heat to the surrounding media by conduction or other means becomes negligible with increasing fracture velocity. Hence, any heat that is generated is entrapped in the dissipation zone of a propagating crack.

Therefore, viewing these irreversible phenomena at this localized scale rather than on a bulk basis, it would appear that a feasible argument could be made for the need to consider the thermal effects in the study of quasi-brittle fracture propagation. The influence of these effects increasing in significance for fracture velocities of solids approaching the terminal level.

Assuming then the existence of a dissipation zone at the tip of a moving crack, it is the object of this investigation to determine the analytical significance such irreversibilities would have on the behavior of quasi-brittle fracture propagation.

In the Appendix the necessary Green's functions are determined for the evaluation of the thermoelastic stresses present in a wedge-shaped body in which heat is being generated. These results are then applied in the following section to the analysis of a constant velocity crack.

THE ANALYSIS OF A PROPAGATING CRACK

At the tip of a crack a high and very localized region of stress exists. It may be assumed that within this region and proceeding with the crack, plastic work is being done. If these deformation processes are slow, the heat generated by the plastic work is dissipated by conduction throughout the material as it occurs. Consequently the process is considered to be isothermal and no thermal stresses would result. However, as the velocity increases and correspondingly the plastic work rate, the heat as it is generated becomes entrapped. In this case additional stresses are imposed by the process which is now considered to be adiabatic.

For the adiabatic case the effects of the heat generation may be singled out for a thermoelastic evaluation. In this way one may account for the irreversibilities which occur at the crack tip and in turn examine the changes in the elastic stress field which surrounds the propagating crack without formally solving a problem in plasticity.

In the region where the plastic deformations are occurring essentially all of the energy is converted into heat. The only recoverable part is that due to the contained elastic deformations. In general this part is comparatively small and for most engineering materials may be ignored.

Applying then the principle of conservation of energy, the amount of the specific heat energy associated with these deformation processes can be evaluated from the inelastic work as

$$Q_p = \frac{u_p}{J} = \frac{1}{J}\int \sigma_{ij}\, \mathrm{d}\epsilon_{ij}^{p}, \tag{1}$$

where the integral is taken over the actual strain path from some initial state of the material and J is the mechanical equivalent of heat. For the plane problem considered the total heat, Q_p^T, developed as a result of the distributed inelastic work is then,

$$Q_p^T = \int_A Q_p \, \mathrm{d}A, \tag{2}$$

where A is the region of plasticity developed at the crack tip.

At the present time no analytical solution to describe the elastic–plastic deformations for an opening mode crack is available. Hence, neither (1) nor (2) can be formally evaluated. In an attempt to overcome some of these current difficulties we cite McClintock and Irwin's recent publication [5]. In this study the authors present an analysis for obtaining order-of-magnitude estimates of the plasticity effects.

For our thermoelastic analysis of the propagating crack, it is assumed that the heat generated by the region of plastic work may be approximated as an arrangement of instantaneous heat sources. The heat sources are assumed to be uniform in strength and distributed over a small circular region of radius R, centered at the tip of the crack. The actual section may not, in fact, be circular but this measure can be regarded as an equivalent section to the true shape.

Expressed in cylindrical coordinates the line sources of strength q_p are,

$$q_p = \frac{u_p}{J\rho C} r' \, \mathrm{d}r' \, \mathrm{d}\theta' \tag{3}$$

where u_p is the average of the equivalent specific plastic work.

The stresses, resulting from the assumed distribution, are obtained directly from equation (A18) as,

$$\tilde{\sigma}_{ij}(r, \theta, t) = \frac{u_p}{J\rho C} \int_0^{2\pi} \int_0^R \sigma_{ij} r' \, \mathrm{d}r' \, \mathrm{d}\theta'. \tag{4}$$

Similarly, from (A23), one obtains for the asymptotic behavior of the stresses for small r,

$$\begin{aligned}
\tilde{\sigma}_{rr} &= -P \cos\frac{\theta}{2}\left(1 + \sin^2\frac{\theta}{2}\right) r^{-\frac{1}{2}} + O(r^0) \\
\tilde{\sigma}_{\theta\theta} &= -P \cos^3\frac{\theta}{2} r^{-\frac{1}{2}} + O(r^0) \\
\tilde{\sigma}_{r\theta} &= -\tfrac{1}{2} P \sin\theta \cos\frac{\theta}{2} r^{-\frac{1}{2}} + O(r^0) \\
P &= \frac{2E\alpha u_p R^{\frac{1}{2}}}{3\pi(1-\nu) J\rho C} \mathrm{T}\left(\tfrac{3}{2}, 1, \frac{R}{2(\kappa t)^{\frac{1}{2}}}\right)
\end{aligned} \tag{5}$$

with $\mathrm{T}(a, b, z)$ representing the Toronto function.

For the crack, moving at a constant velocity V, both the size and shape of the region of plastic work, as well as the rate of deformation, $\dot{u}_p$, are independent of time. Hence, the resulting quasi-static thermoelastic stress state can be evaluated directly from equations (4) and (5) by the technique described previously in conjunction with equation (A24). In this way the stresses near the region of heat generation are found to be,

$$\begin{aligned}
\sigma^*_{rr} &= -P^* \int_0^\infty \rho^{-\frac{1}{4}} (\rho_1 + \rho_2)^{\frac{1}{2}} (3\rho_1 - \rho_2) \rho_1^{-2} {}_1F_1(\tfrac{3}{4}, 2, -a\rho) \, \mathrm{d}\rho \\
\sigma^*_{\theta\theta} &= -P^* \int_0^\infty \rho^{-\frac{1}{4}} (\rho_1 + \rho_2)^{\frac{3}{2}} \rho_1^{-2} {}_1F_1(\tfrac{3}{4}, 2, -a\rho) \, \mathrm{d}\rho \\
\sigma^*_{r\theta} &= -P^* \int_0^\infty \rho^{\frac{3}{4}} \sin\theta (\rho_1 + \rho_2)^{\frac{1}{2}} \rho_1^{-2} {}_1F_1(\tfrac{3}{4}, 2, -a\rho) \, \mathrm{d}\rho \\
a &= Vt^*/r, \qquad t^* = R^2/4\kappa, \\
\rho_1^2 &= \rho^2 - 2\rho\cos\theta + 1, \qquad \rho_2 = \rho\cos\theta - 1, \\
P^* &= \frac{\Gamma(\frac{5}{4}) E\alpha \dot{u}_p R^{\frac{1}{2}} t^*}{3 \,.\, 2^{\frac{1}{2}} \pi(1-\nu) J\rho C r^{\frac{1}{2}} a^{\frac{1}{4}}}.
\end{aligned} \tag{6}$$

Completing the integration of $\sigma_{\theta\theta}^*$ for $y = 0$ one obtains,

$$\sigma_{\theta\theta}^* = -2^{\frac{3}{2}}P^*\left\{\frac{\Gamma^2(\frac{1}{4})}{\pi^{\frac{1}{2}}}\,{}_2F_2(\tfrac{1}{4},\tfrac{3}{4};2,\tfrac{3}{4};a_0) - \frac{4^3 a_0^{\frac{1}{4}}}{5\Gamma(\frac{1}{4})}\,{}_2F_2(\tfrac{1}{2},1;\tfrac{9}{4},\tfrac{5}{4};a_0)\right\},$$
$$a_0 = Vt^*/x. \tag{7}$$

where V is the velocity of the crack moving in the direction of the positive x-axis.

As the fracture velocity increases with respect to the material's characteristic thermal time (t^*) the stress, determined by equation (7), approaches as an asymptotic limit

$$\sigma_{\theta\theta}^* = -\frac{2\Gamma^2(\frac{1}{4})E\alpha\dot{u}_p t^* R^{\frac{1}{2}}}{9\Gamma^2(\frac{3}{4})\pi^{\frac{1}{2}}(1-\nu)J\rho C a_0^{\frac{1}{2}} x^{\frac{1}{2}}}. \tag{8}$$

It is convenient at this point to compute a quantity useful in photoelastic analysis; specifically, the difference of the principal stresses, which is proportional to the isochromatic lines. Thus, near the region of heat generation,

$$\begin{aligned}\sigma_1^* - \sigma_2^* &= [(\sigma_{rr}^* - \sigma_{\theta\theta}^*)^2 + 4\sigma_{r\theta}^{*2}]^{\frac{1}{2}} \\ &= -2^{\frac{3}{2}}P^*\int_0^\infty \rho^{\frac{1}{4}}\sin\theta\,\rho_1^{-\frac{3}{2}}\,{}_1F_1(\tfrac{3}{4},2,-a\rho)\,\mathrm{d}\rho.\end{aligned} \tag{9}$$

Completing the integration of (9) results in,

$$\sigma_1^* - \sigma_2^* = -\frac{\Gamma^2(\frac{1}{4})E\alpha\dot{u}_p t^* R^{\frac{1}{2}}}{6\Gamma(\frac{3}{4})\pi^{\frac{1}{2}}(1-\nu)J\rho C r^{\frac{1}{2}}(2a)^{\frac{1}{4}}}\cdot\frac{\sin\theta}{(\cos\theta+1)^{\frac{1}{4}}}\sum_{n=0}^{\infty}\frac{P_n^{\frac{1}{4},-\frac{1}{4}}(\cos\theta)}{2_n}a^n, \qquad |\theta| < \pi. \tag{10}$$

NUMERICAL RESULTS AND DISCUSSION

For a body in which heat is being conducted there is no thermal wave velocity to which one can attach a meaning. Therefore, instead of a wave velocity, one uses as a reference parameter the materials characteristic thermal time, t^*. This being the time required for the temperature at a point distant r from a source of heat to attain its maximum value. In the case of an infinite body subjected to an instantaneous line source, as considered in this investigation, the thermal time t^* is $r^2/4\kappa$.

In the analysis of the fracturing process it was assumed that the rate of heat generation by plastic deformation is equal to or greater than the rate of heat removal by conduction. To characterize this adiabatic process we define then, in addition to the thermal time t^*, the mechanical time $\bar{t}$, where $\bar{t} = r/V$. Hence, by the ratio of $t^*/\bar{t}$, one can examine the effects of increased fracture velocity, here decreased mechanical time, for a particular material's characteristic thermal time.

To establish the state of stress in the material as a function of the fracture velocity, it is further assumed that the rate of deformation, $\dot{u}_p$, occurring at the tip of a constant velocity crack, is proportional to the crack velocity, as

$$\dot{u}_p = \frac{u_p}{2R}V \tag{11}$$

where u_p is the average equivalent of the specific plastic work.

Hence, incorporating the definition for the adiabatic time ratio and the above assumption (11), we can express equation (7) for $y = 0$ in the form,

$$\sigma^*_{\theta\theta} = \frac{-K^*}{(2\pi)^{\frac{1}{2}}} r^{-\frac{1}{2}} \tag{12}$$

where

$$K^* = \frac{\Gamma(\frac{1}{4}) E\alpha u_p R^{\frac{1}{2}} A_0^{\frac{3}{4}}}{6(2\pi)^{\frac{1}{2}}(1-\nu) J\rho C}$$

$$\cdot \left\{ \frac{\Gamma^2(\frac{1}{4})}{\pi^{\frac{1}{2}}} {}_2F_2(\tfrac{1}{4}, \tfrac{3}{4}; \tfrac{3}{4}, 2; A_0) - \frac{4^3 A_0^{\frac{1}{4}}}{5\Gamma(\frac{1}{4})} {}_2F_2(\tfrac{1}{2}, 1; \tfrac{5}{4}, \tfrac{9}{4}; A_0) \right\},$$

and

$$A_0 = \left(\frac{t^*}{\bar{t}} \right)_{r=R}.$$

The asymptotic limit of the stress intensity factor, K^*, as established in equation (8) for $A_0 \gg$, is then

$$K^* = \frac{2^{\frac{1}{2}} \Gamma^2(\frac{1}{4}) E\alpha u_p A_0^{\frac{1}{2}} R^{\frac{1}{2}}}{9\Gamma^2(\frac{3}{4})(1-\nu) J\rho C}. \tag{13}$$

The behavior of equations (12) and (13) as a function of A_0 is displayed in Fig. 1. In this nondimensional plot we find that as the material's crack velocity increases, the magnitude of the stress, $-\sigma^*_{\theta\theta}$ also increases in size.

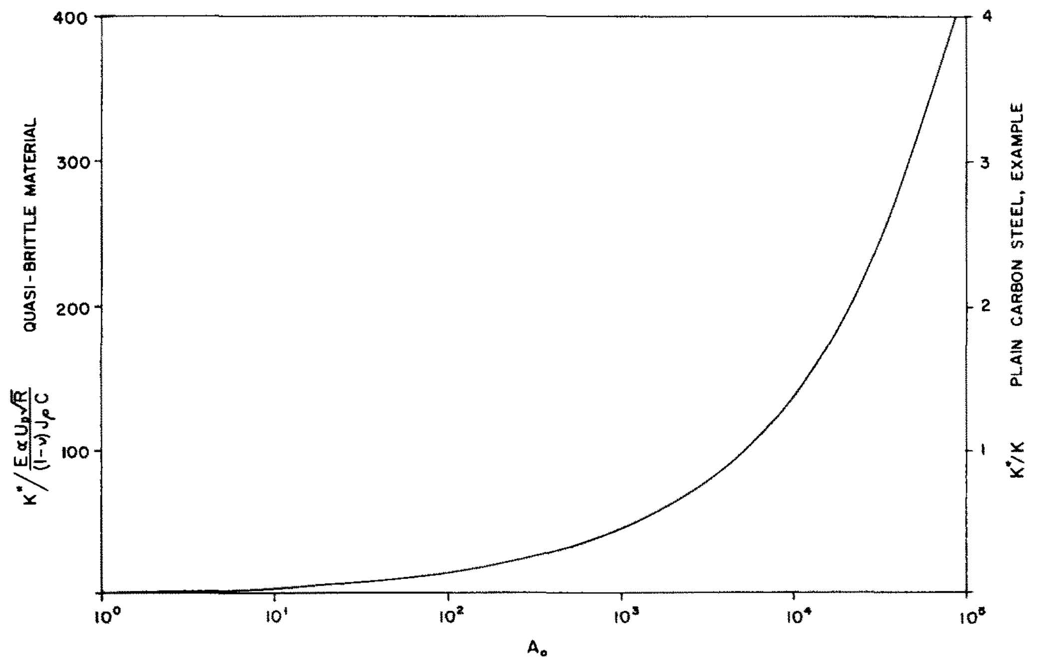

FIG. 1. Nondimensional plot of stress intensity factor, K^* vs. adiabatic crack velocity parameter, A_0.

If it is assumed that the radius, R, of the region of heat input can be estimated by Irwin's plastic zone approximation [4],

$$R = \frac{1}{2\pi}\left(\frac{K}{\sigma_{ys}}\right)^2 \tag{14}$$

then the ordinate of Fig. 1 can also be expressed as a ratio of K^*/K with a scale factor equaling $[E\alpha u_p/(2\pi)^{\frac{1}{2}}(1-\nu)J\rho C\sigma_{ys}]$. In this case, to examine the order-of-magnitude variation that K^*/K would have for a real solid, we consider as an example a material such as plain carbon steel. Here the approximate values of E, ν, α, and σ_{ys} are taken to be 30×10^6 psi, 0·3, 6×10^{-6} in./in./°F and 100 ksi respectively. Assuming that for this material the average temperature rise occurring within the plastic zone for all crack velocities is of the order 10°F, then the typical range of values K^*/K vs. A_0 would attain is as given on the right hand ordinate of Fig. 1. If it is desired to compare K^*/K with V, the crack velocity, the approximate radius of the equivalent region of heat input and the materials thermal diffusivity must be known. By multiplying A_0 by the scale factor $4\kappa/R$ the abscissa then represents the corresponding velocity of fracture of the material.

In equation (10) it was established that the isochromatics for a moving source of heat are of the form

$$n \sim r^{-\frac{1}{2}} A_0^{-\frac{1}{4}} \frac{\sin\theta}{(\cos\theta+1)^{\frac{1}{4}}} \sum_{m=0}^{\infty} \frac{P_m^{\frac{1}{4},-\frac{1}{4}}\cos\theta}{2_m} A_0^m, \qquad |\theta| < \pi. \tag{15}$$

In Fig. 2 the shape of these isochromatics for three values of A_0 are presented.

From these results it appears that the influence of the region of plasticity on the elastic field surrounding a running crack would be to modify the oncoming region while leaving the trailing area relatively unchanged. If one knew the relative magnitudes of the isochromatics for both elastic cases, i.e., that which is causing the crack to run and that which is due to the resulting heat generation, then superposition could be used to obtain an approximate form of the isochromatics for a running crack. At the present level of understanding, these magnitudes can only be conjectured. However, it does seem reasonable to point out that the photographs of the isochromatic fringes as reported by Wells and Post [6] and more recently van Elst [7] do appear to have modifications in their shape at the tip of the propagating crack similar to that indicated in Fig. 2.

By assuming the presence of plastic work at the tip of a propagating crack it has been possible to separate out the influence of this irreversibility from an existing crack driving stress field. In this way we have been able to show that the stresses immediately preceding the propagating crack are reduced in intensity as a natural consequence of a materials irreversibility. Further, the magnitude of this reduction increases with increasing crack velocity.

Continuing in the framework of our quasi-static analysis, it may be assumed that the stress field for a running crack in the absence of plastic work is the same as that for the elasto-static problem having the same crack length. Beyond the crack-border plastic zone then, the tensile stress normal to the plane of expected crack propagation is, by superposition,

$$\sigma_{\theta\theta} = (K - K^*)/(2\pi r)^{\frac{1}{2}}. \tag{16}$$

Hence the stress intensity factor normally associated with material evaluation can now be separated into two distinct parts. In this way, the fracture energy's two main components,

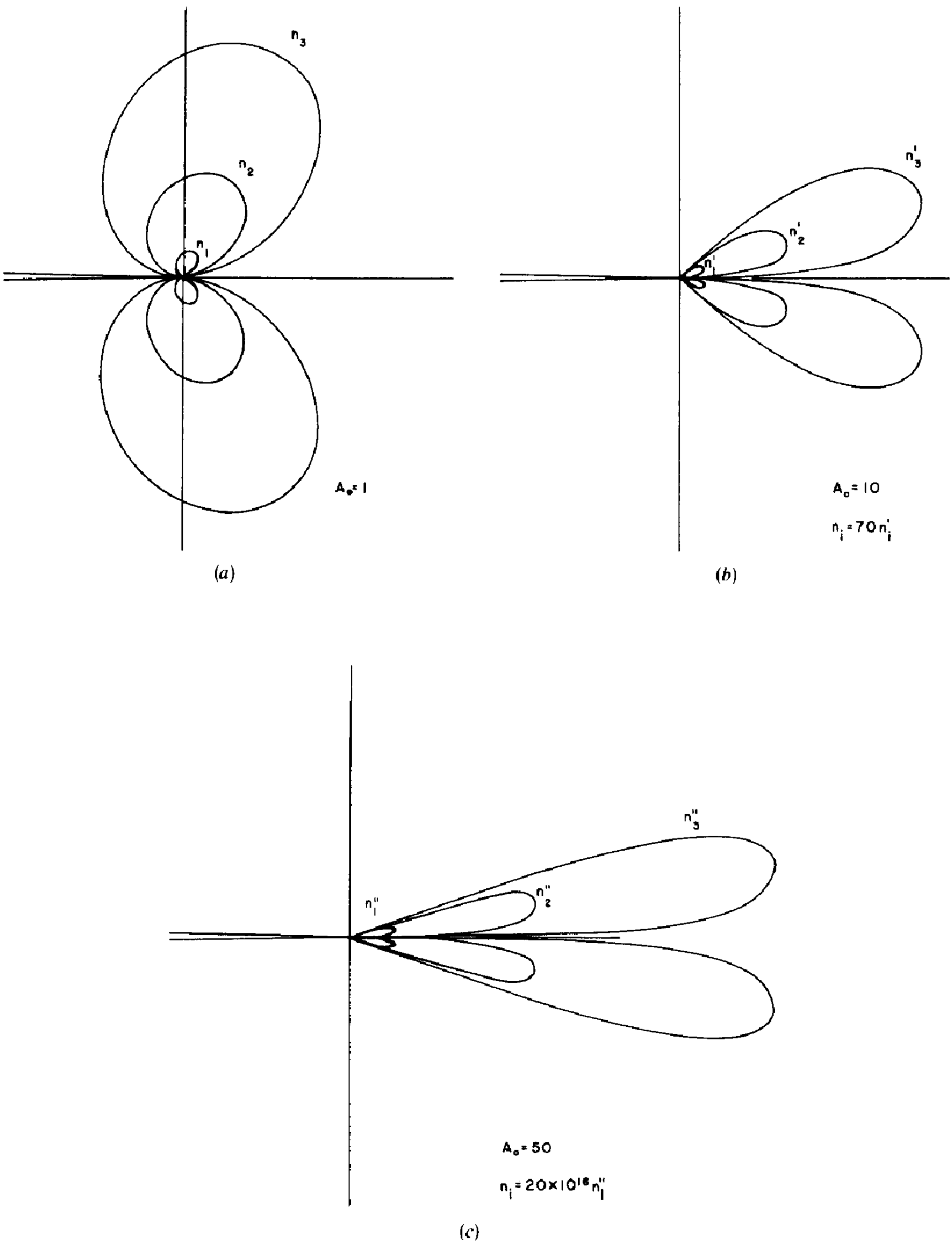

FIG. 2. Isochromatic-fringe patterns

$$n \sim r^{-\frac{1}{2}} A_0^{-\frac{1}{2}} \frac{\sin\theta}{(\cos\theta+1)^{\frac{1}{2}}} \sum_{m=0}^{\infty} \frac{P_m^{\frac{1}{2},-\frac{1}{2}}\cos\theta}{2_m} A_0^m, \quad |\theta| < \pi.$$

namely the conventional surface energy of the solid and the dissipation energy caused by the irreversible phenomena occurring in the dissipation zone around the periphery of the propagating crack, can be ascribed to two individual and independent stress intensity factors.

The elastic stress analysis of the crack border given by equation (16) applies only to crack velocities for which adiabatic conditions exist in the plastic zone. Hence, as thermal diffusivity increases and/or the plastic zone size decreases, larger crack velocities are necessary for adiabatic conditions to exist. Evidence to the effect was given in 1963 by Irwin [8]. In this report he indicated that by an estimate of an isothermal–adiabatic velocity boundary, one can predict the approximate crack velocity at which increasing material toughness occurs.

To examine how well equation (16) predicts actual material behavior we refer to the data from the University of Illinois wide plate test results [9, 10] and the further report of this work by Eftis and Krafft [11]. In making the comparison, the value of K is taken to be equivalent to the materials reported minimum toughness for adiabatic propagation, $K_I = 37\ \mathrm{ksi}\sqrt{\mathrm{in}}$. The value of K^* is then based on this value of K, considering K to be a material constant at the larger velocities of propagation. As before, E, ν, and α are assumed to be 30×10^6 psi, 0·3, and 6×10^{-6} in./in./°F respectively. R, the equivalent radius of the heat input zone is assumed equal to 0·0185 in., the reported value in reference [11] of the minimum adiabatic plastic zone size for the test material at −12°F. Corresponding to this zone size and in line with the estimates of reference [11], the average temperature rise occurring at the crack tip is taken as approximately 20°F. The thermal diffusivity, κ, for this material at −12°F is estimated from reference [12] to be 0·028 in^2/sec.

In Fig. 3 is presented a nondimensional comparison between the predicted increase in material toughness K^*/K and the actual material behavior $(\tilde{K}-K)/K$ vs. A_0. $\tilde{K}$ are the

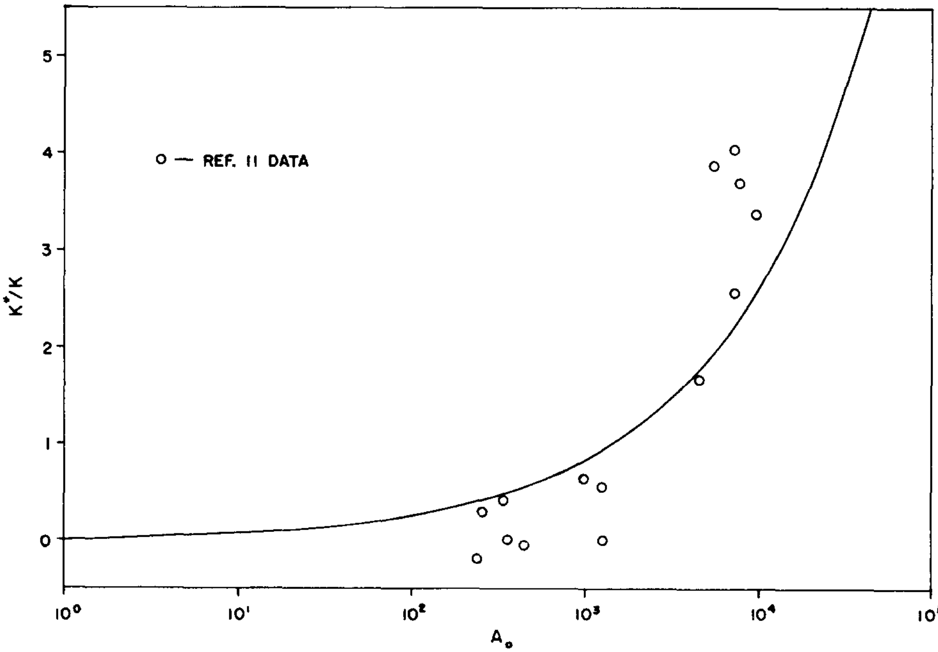

FIG 3. K^*/K vs. A_0 for a mild steel.

reported values of the University of Illinois wide plate test results as found in reference [11], Table 1. Although the numerical estimates used for the parameters in arriving at the curve of Fig. 3 must, without experimental verification, be considered as order-of-magnitude approximations, the analysis does appear capable of predicting the resulting changes in material toughness with fracture velocity. Furthermore, the plausibility of these estimates indicates that the parameters of K^* are significant factors in determining the behavior of a material in the adiabatic range of fracture velocities.

In conclusion, it may be stated that the presence of the compressive thermal stresses at the crack tip tend to reduce the stress intensity for cleavage and increase the fracture resistance of the solid. This being a natural consequence of a materials irreversibility. Likewise, with these thermal effects taken into account, it is not difficult to explain why at the high fracture velocities, crack extension is a stable process in the sense that if the K_{total} value could be maintained constant the crack speed would also remain constant.

Acknowledgement—This study was conducted while the author was a National Research Council—Postdoctoral Resident Research Associate at the U.S. Naval Research Laboratory, Washington, D.C. The author is indebted to G. R. Irwin for his suggestion of the problem and his comments and support throughout the course of its development.

REFERENCES

[1] F. ERDOGAN, Crack propagation theories. *Rep. Dep. Mech. Lehigh Univ.* (1967).
[2] C. ZENER and J. H. HOLLOMON, Effect of strain rate upon plastic flow of steel. *J. appl. Phys.* **15**, 22 (1944).
[3] A. NADAI, *Theory of Flow and Fracture of Solids*, Vol. II. McGraw-Hill (1963).
[4] A. M. SULLIVAN, Unpublished results.
[5] F. A. McCLINTOCK and G. R. IRWIN, Plasticity aspects of fracture mechanics. *Symp. Fracture Toughness Testing and Its Applications*, p. 48. ASTM (1965).
[6] A. A. WELLS and D. POST, The dynamic stress distribution surrounding a running crack. *Proc. Soc. exp. Stress Analysis* **16**, 69 (1958).
[7] H. C. VAN ELST, The intermittent propagation of brittle fracture in steel. *Trans. Am. Inst. mech. Engrs* **230**, 460 (1964).
[8] G. R. IRWIN, Crack-toughness testing of strain-rate sensitive materials. *Trans. Am. Soc. mech. Engrs* **86**, A, 444 (1964).
[9] F. F. VIDEON, F. W. BARTON, and W. J. HALL, Brittle fracture studies. Civil Engineering Studies, Structural Research Series No. 255, University of Illinois, Urbana, Ill.
[10] F. F. VIDEON, F. W. BARTON and W. J. HALL, Brittle fracture propagation studies. Ship Structure Committee Report SSC-148, Aug. 1963, Office of Technical Services, Wash., D.C., 20230.
[11] J. EFTIS and J. M. KRAFFT, A comparison of the initiation with the rapid propagation of a crack in a mild steel plate. *Trans. Am. Soc. mech. Engrs* **87**, B, 257 (1965).
[12] A. GOLDSMITH, T. E. WATERMAN and H. J. HIRSCHHORN, *Handbook of Thermophysical Properties of Solid Materials*. Macmillan (1961).
[13] W. NOWACKI, *Thermoelasticity*. Addison-Wesley (1962).
[14] C. K. YOUNGDAHL and E. STERNBERG, Transient thermal stresses in a circular cylinder. *J. appl. Mech.* **28**, 25 (1961).
[15] E. STERNBERG and J. G. CHAKRAVORTY, On inertia effects in a transient thermoelastic problem. *J. appl. Mech.* **26**, 503 (1959).
[16] H. S. CARSLAW and J. C. JAEGER, *Conduction of Heat in Solids*, 2nd edition. Cambridge University Press (1959).
[17] R. A. LUCAS and F. ERDOGAN, Quasi-static transient thermal stresses in an infinite wedge. *Int. J. Solids Struct.* **2**, 205 (1966).

APPENDIX

THERMAL STRESSES IN AN INFINITE WEDGE

In the following section we consider a wedge of an arbitrary angle having stress-free boundaries and subjected to a heat pulse. The principal objective is to establish the Green's functions for the stress analysis of a wedge with time-dependent heat generation.

In this analysis the inertia effects are neglected. Hence, depending on the time variation of the heat input investigated, one may need to consider the magnitude of the ignored inertia effects. In many cases of thermal loading these effects are small and their neglect is justified. Examples of this can be found in the recent studies of dynamic thermoelasticity, [13, 14, 15].

Largely for mathematical expediency, also ignored in this section are the effects of temperature on the thermoelastic constants along with the thermoelastic coupling and the anelastic behavior of the material.

The heat conduction and equilibrium equations, expressed in terms of displacements in cylindrical coordinates, are

$$\frac{\partial^2 T}{\partial r^2}+\frac{1}{r}\frac{\partial T}{\partial r}+\frac{1}{r^2}\frac{\partial^2 T}{\partial \theta^2}+\frac{q}{K'} = \frac{1}{\kappa}\frac{\partial T}{\partial t} \tag{A1}$$

$$\begin{aligned}(\lambda+2\mu)\frac{\partial e}{\partial r}-\frac{2\mu}{r}\frac{\partial \omega_z}{\partial \theta}-(3\lambda+2\mu)\alpha\frac{\partial T}{\partial r} &= 0\\ (\lambda+2\mu)\frac{1}{r}\frac{\partial e}{\partial \theta}+2\mu\frac{\partial \omega_z}{\partial r}-(3\lambda+2\mu)\frac{\alpha}{r}\frac{\partial T}{\partial \theta} &= 0\end{aligned} \tag{A2}$$

where K' is the coefficient of heat conduction, q is the heat generated in a unit volume and unit time, κ is the coefficient of diffusivity. λ and μ are Lamé's constants, α is the coefficient linear thermal expansion, T is the temperature and the dilatation e and the rotation ω_z, in this coordinate system, are as follows:

$$e = \frac{\partial(ru)}{r\partial r}+\frac{\partial v}{r\partial \theta}, \qquad \omega_z = \frac{1}{2r}\left(\frac{\partial(rv)}{\partial r}-\frac{\partial u}{\partial \theta}\right). \tag{A3}$$

Consider now an infinite wedge, $r > 0$, $-\beta \leq \theta \leq \beta$ subject to the following initial and boundary conditions

$$\begin{aligned}&T(r,\theta,t) = 0, \qquad t \leq 0\\ &\frac{\partial T(r,\theta,t)}{\partial \theta} = 0, \qquad \theta = \pm\beta, \qquad t > 0\\ &q(r,\theta,t) = Q\frac{1}{r}\delta(r-r')\delta(\theta-\theta')\delta(t-t').\end{aligned} \tag{A4}$$

$$\begin{aligned}&\sigma_{ij}(r,\theta,t) = 0, \qquad t \leq 0, \qquad (i,j = r,\theta)\\ &\sigma_{\theta\theta}(r,\theta,t) = 0, \qquad \sigma_{r\theta}(r,\theta,t) = 0, \qquad \theta = \pm\beta, \qquad t > 0\end{aligned} \tag{A5}$$

where Q is the intensity of the heat source (Btu per unit thickness).

The solution of (A1) subject to (A4), for an instantaneous point source and wedge angle taken as $0 \leq \theta \leq \theta_0$, was obtained by Carslaw and Jaeger [16]. Expressing their result for a line source in the wedge $-\beta \leq \theta \leq \beta$ and selecting only the symmetric part of the solution corresponding to heat sources of strength $q_0/2$ at $r = r'$ and $\theta = \pm\theta'$, we obtain

$$
\begin{aligned}
T &= \frac{q_0}{4\kappa\beta t}\exp\left(-\frac{r^2+r'^2}{4\kappa t}\right)\cdot\left\{I_0\left(\frac{rr'}{2\kappa t}\right)+2\sum_{n=0}^{\infty} I_k\left(\frac{rr'}{2\kappa t}\right)\cos k\theta' \cos k\theta\right\} \\
k &= (n+1)\pi/\beta \qquad q_0 = Q/\rho C
\end{aligned} \tag{A6}
$$

where ρ is the density and C the specific heat. The symmetric part is selected in anticipation of the physical problem to be evaluated. For the more general solution of an arbitrarily located source one need only include, by superposition, the ignored anti-symmetric component of the temperature.

To solve (A2) we will use successively Mellin–Laplace transformations in variables r and t. For a given suitably well-behaved function $f(r, t)$ the Mellin–Laplace transform pairs are formally defined as

$$
\begin{aligned}
\hat{\hat{f}}(p, s) &= \int_0^{\infty} e^{-st}\,dt \int_0^{\infty} f(r, t) r^{p-1}\,dr \\
f(r, t) &= \frac{1}{2\pi i}\int_{c-i\infty}^{c+i\infty} r^{-p}\,dp\,\frac{1}{2\pi i}\int_{\gamma-i\infty}^{\gamma+i\infty} \hat{\hat{f}}(p, s)\,e^{st}\,ds.
\end{aligned} \tag{A7}
$$

Taking into account the initial conditions, assuming that within the strip of regularity containing the Bromwitch line of the Mellin inversion integral the functions T, u and v are such that

$$
r^pT,\ r^{p-1}u,\ r^p\frac{\partial u}{\partial r},\ r^{p-1}\frac{\partial u}{\partial \theta},\ r^{p-1}v,\ r^p\frac{\partial v}{\partial r},\ r^{p-1}\frac{\partial v}{\partial \theta} \to 0
$$

as (A8)

$$
r \to 0 \quad \text{and} \quad r \to \infty
$$

and integrating by parts, from (A2) and (A3) we obtain

$$
\begin{aligned}
&\frac{d^2\hat{\hat{u}}}{d\theta^2} + B_1\frac{d\hat{\hat{v}}}{d\theta} + B_2\hat{\hat{u}} + B_3\hat{\hat{T}} = 0 \\
&\frac{d^2\hat{\hat{v}}}{d\theta^2} + B_4\frac{d\hat{\hat{u}}}{d\theta} + B_5\hat{\hat{v}} - B_6\frac{d\hat{\hat{T}}}{d\theta} = 0
\end{aligned} \tag{A9}
$$

where $\hat{\hat{T}}$, $\hat{\hat{u}}$, $\hat{\hat{v}}$ are, respectively, the Mellin–Laplace transforms of T, $r^{-1}u$ and $r^{-1}v$ and the constants are given by

$$
\begin{aligned}
&B_1 = -2-\frac{A}{\mu}p+p \qquad B_2 = \frac{A}{\mu}p(p-2) \qquad B_3 = \frac{k^*p}{\mu} \\
&B_4 = 2+\frac{\mu}{A}p-p \qquad B_5 = \frac{\mu}{A}p(p-2) \qquad B_6 = \frac{k^*}{A} \\
&A = \lambda+2\mu \qquad k^* = (3\lambda+2\mu)\alpha.
\end{aligned} \tag{A10}
$$

In a similar way the Mellin–Laplace transforms of the boundary and initial conditions, (A5), and the symmetric temperature field, (A6), become

$$A\left(\hat{\hat{u}}+\frac{\mathrm{d}\hat{\hat{v}}}{\mathrm{d}\theta}\right)-\lambda(p-1)\hat{\hat{u}}-k^*\hat{\hat{T}}=0,\ \frac{\mathrm{d}\hat{\hat{u}}}{\mathrm{d}\theta}-p\hat{\hat{v}}=0, \qquad \theta=\pm\beta \tag{A11}$$

$$\hat{\hat{T}}=\frac{q_0}{\beta}\left\{\hat{\hat{F}}_0+2\sum_{n=0}^{\infty}\hat{\hat{F}}_k\cos k\theta'\cos k\theta\right\}, \tag{A12}$$

where

$$\hat{\hat{F}}_\zeta(p,s)=\int_0^\infty \mathrm{e}^{-st}\,\mathrm{d}t\int_0^\infty\frac{1}{4\kappa t}\exp\left(-\frac{r^2+r'^2}{4\kappa t}\right)I_\zeta\left(\frac{rr'}{2\kappa t}\right)r^{p-1}\,\mathrm{d}r, \qquad \zeta=0,k. \tag{A13}$$

The solution of the domain equations (A9), subject to the temperature distribution (A12) and the boundary conditions (A11), after some algebra results in the Mellin–Laplace transforms of the displacements u and v.

In the expressions thereby found for $\hat{\hat{u}}$ and $\hat{\hat{v}}$, it is noted that the Laplace parameter appears only through $\hat{\hat{F}}_\zeta(p,s)$. Hence, the Mellin transforms of the displacements are obtained by simply replacing $\hat{\hat{F}}_\zeta$ by $\bar{F}_\zeta$, which is given by

$$\bar{F}_\zeta(p,t)=\frac{1}{4\kappa t}\int_0^\infty\exp\left(-\frac{r^2+r'^2}{4\kappa t}\right)I_\zeta\left(\frac{rr'}{2\kappa t}\right)r^{p-1}\,\mathrm{d}r, \qquad \zeta=0,k. \tag{A14}$$

Through this Laplace inversion, the Mellin transforms of the stresses are obtained as,

$$\begin{aligned}
\bar{\sigma}_{rr}&=\frac{q_0E\alpha(p-2)}{\beta(1-\nu)G(p,\beta)}\left\{\left[\frac{\bar{F}_0}{(p-2)^2}+2\sum_{n=0}^{\infty}\frac{(-1)^n\bar{F}_k\cos k\theta'}{k^2-(p-2)^2}\right]\right.\\
&\quad.\,[(p-1)(p+2)\sin(p-2)\beta\cos p\theta-p(p-1)\sin p\beta\cos(p-2)\theta]\\
&\quad\left.+\frac{G(p,\beta)}{(p-2)}\left[\frac{\bar{F}_0}{(p-2)}-2\sum_{n=0}^{\infty}\frac{(k^2+p-2)\bar{F}_k\cos k\theta'\cos k\theta}{k^2-(p-2)^2}\right]\right\},\\
\bar{\sigma}_{\theta\theta}&=\frac{q_0E\alpha(p-2)}{\beta(1-\nu)G(p,\beta)}\left\{\left[\frac{\bar{F}_0}{(p-2)^2}+2\sum_{n=0}^{\infty}\frac{(-1)^n\bar{F}_k\cos k\theta'}{k^2-(p-2)^2}\right]\right.\\
&\quad.\,[p(p-1)\sin p\beta\cos(p-2)\theta-(p-1)(p-2)\sin(p-2)\beta\cos p\theta]\\
&\quad\left.-(p-1)G(p,\beta)\left[\frac{\bar{F}_0}{(p-2)^2}-2\sum_{n=0}^{\infty}\frac{\bar{F}_k\cos k\theta'\cos k\theta}{k^2-(p-2)^2}\right]\right\},\\
\bar{\sigma}_{r\theta}&=\frac{q_0E\alpha(p-2)}{\beta(1-\nu)G(p,\beta)}\left\{\left[\frac{\bar{F}_0}{(p-2)^2}+2\sum_{n=0}^{\infty}\frac{(-1)^n\bar{F}_k\cos k\theta'}{k^2-(p-2)^2}\right]\right.\\
&\quad.\,[p(p-1)\sin(p-2)\beta\sin p\theta-p(p-1)\sin p\beta\sin(p-2)\theta]\\
&\quad\left.-\frac{2(p-1)G(p,\beta)}{(p-2)}\sum_{n=0}^{\infty}\frac{k\bar{F}_k\cos k\theta'\sin k\theta}{k^2-(p-2)^2}\right\},\\
G(p,\beta)&=(p-1)\sin 2\beta+\sin 2(p-1)\beta.
\end{aligned} \tag{A15}$$

The stresses are obtained by using the Mellin inversion theorem:

$$\sigma_{ij}(r, \theta, t) = \frac{1}{2\pi i}\int_{c-i\infty}^{c+i\infty} \bar{\sigma}_{ij}(p, \theta, t)r^{-p}\,\mathrm{d}p, \qquad (i, j = r, \theta). \tag{A16}$$

Equations (A15) indicate that, since the Mellin inversion of $\bar{F}_\zeta$ is known, by writing

$$\bar{\sigma}_{ij}(p, \theta, t) = \bar{F}_0(p, t)\bar{\tau}_{ij}(p, \theta) + \sum_{n=0}^{\infty} \bar{F}_k(p, t)\bar{\tau}_{ijn}(p, \theta), \qquad (i, j = r, \theta), \tag{A17}$$

the stresses may be obtained as an infinite series of convolution integrals:

$$\sigma_{ij}(r, \theta, t) = \int_0^\infty F_0(r/\rho, t)\tau_{ij}(\rho, \theta)\frac{\mathrm{d}\rho}{\rho} + \sum_{n=0}^{\infty}\int_0^\infty F_k(r/\rho, t)\tau_{ijn}(\rho, \theta)\frac{\mathrm{d}\rho}{\rho} \tag{A18}$$

where

$$F_\zeta(r, t) = \frac{1}{4\kappa t}\exp\left(-\frac{r^2+r'^2}{4\kappa t}\right)I_\zeta\left(\frac{rr'}{2\kappa t}\right), \qquad \zeta = 0, k \tag{A19}$$

and τ_{ij}, τ_{ijn} $(i, j = r, \theta; n = 0, 1, 2, \ldots)$ are the inversions of $\bar{\tau}_{ij}$, $\bar{\tau}_{ijn}$, which are the coefficients of the $\bar{F}_\zeta$ as established in (A15).

By examination of the $\bar{\sigma}_{ij}$, it is found that within the strip $\frac{1}{2} < \mathscr{R}(p) < \frac{3}{2}$ the functions remain regular and satisfy conditions (A8). Hence, by taking the line of integration at $c = 1$ and writing $p = 1+iy$, τ_{ij} and τ_{ijn} may be expressed in terms of real integrals as:

$$\begin{aligned}
\tau_{rr} = {} & \frac{q_0 E\alpha}{\pi\beta(1-\nu)}\int_0^\infty [r(1+\eta^2)N_1]^{-1} \\
& .\{\eta[3\eta M_1 - M_2 - N_1]\sin(\eta\log r) \\
& + [\eta(2-\eta^2)M_1 + \eta^2 M_2 - N_1]\cos(\eta\log r)\}\,\mathrm{d}\eta \\[1ex]
\tau_{rrn} = {} & \frac{2q_0 E\alpha\cos k\theta'}{\pi\beta(1-\nu)}\int_0^\infty (rN_1N_2)^{-1} \\
& .\{[(-1)^n\eta(\eta^2-k^2+1)M_2 - (-1)^n\eta^2(k^2+3\eta^2+3)M_1 \\
& + \eta(k^2-\eta^2-1)N_1]\sin(\eta\log r) \\
& + [(-1)^n\eta(2k^2+k^2\eta^2+\eta^4-\eta^2-2)M_1 - (-1)^n\eta^2(k^2+\eta^2+1)M_2 \\
& - (k^4-2k^2+k^2\eta^2+\eta^2+1)N_1]\cos(\eta\log r)\}\,\mathrm{d}\eta \\[1ex]
\tau_{\theta\theta} = {} & \frac{q_0 E\alpha}{\pi\beta(1-\nu)}\int_0^\infty [r(1+\eta^2)N_1]^{-1}\eta[N_1 - M_2 - \eta M_1] \\
& .[\sin(\eta\log r) - \eta\cos(\eta\log r)]\,\mathrm{d}\eta \\[1ex]
\tau_{\theta\theta n} = {} & \frac{2q_0 E\alpha\cos k\theta'}{\pi\beta(1-\nu)}\int_0^\infty \eta(\eta^2+1-k^2)(rN_1N_2)^{-1}[(-1)^n(M_2+\eta M_1) \\
& + N_1\cos k\theta].[\sin(\eta\log r) - \eta\cos(\eta\log r)]\,\mathrm{d}\eta.
\end{aligned} \tag{A20}$$

$$\tau_{r\theta} = \frac{q_0 E\alpha}{\pi\beta(1-\nu)} \int_0^\infty \eta M_3[r(1+\eta^2)N_1]^{-1}$$
$$.\,[(\eta^2-1)\sin(\eta\log r)+2\eta\cos(\eta\log r)]\,d\eta$$

$$\tau_{r\theta n} = \frac{2q_0 E\alpha\cos k\theta'}{\pi\beta(1-\nu)} \int_0^\infty [(-1)^n\eta(\eta^2+1)M_3+k\eta N_1\sin k\theta](N_1N_2r)^{-1}$$
$$[(1-k^2-\eta^2)\sin(\eta\log r)-2\eta\cos(\eta\log r)\,d\eta$$

$$M_1 = \sin(\beta-\theta)\cosh(\beta+\theta)\eta+\sin(\beta+\theta)\cosh(\beta-\theta)\eta$$

$$M_2 = \cos(\beta-\theta)\sinh(\beta+\theta)\eta+\cos(\beta+\theta)\sinh(\beta-\theta)\eta$$

$$M_3 = \sin(\beta+\theta)\sinh(\beta-\theta)\eta-\sin(\beta-\theta)\sinh(\beta+\theta)\eta$$

$$N_1 = \eta\sin 2\beta+\sinh 2\beta\eta$$

$$N_2 = [\eta^2+(k+1)^2][\eta^2+(k-1)^2]$$

$$k = (n+1)\pi/\beta.$$

For $r < 1$ (A15) may be inverted through the use of the residue theorem by completing the contour in the half plane $\mathscr{R}(p) < 1$. If the behavior of the stresses in the vicinity of the apex of the wedge is of primary interest, we need to examine merely the asymptotic behavior of these inversions for small values of r. The leading terms in the asymptotic expansion of the stresses will be contributed by the residues at those poles of $\bar{\sigma}_{ij}$ which lie closest to the line $\mathscr{R}(p) = c = 1$.

It can be shown that at the zeros of $k^2-(p-2)^2$ the integrands remain regular and therefore are not the locations of poles. Hence, the remaining singularities will occur at the zeros of $G(p, \beta)$ and may be obtained from

$$G = (p-1)\sin 2\beta+\sin 2(p-1)\beta = 0, \qquad p = \varphi_1, \varphi_2, \ldots \tag{A21}$$

A discussion of the distribution of the zeros φ_i of G has been given previously [17]. It suffices to indicate that in the evaluation of the singular behavior of the stresses only φ_1, the largest algebraic singularity, is of importance.

With the location of the singularities thus established the evaluation of the leading terms of the τ_{ij} and τ_{ijn} may be made. Since the configuration of primary interest in this investigation is the semi-infinite crack, ($\beta = \pi$; $\varphi_1 = \frac{1}{2}$), only this result is reported. From the residue theorem it follows that

$$\begin{aligned}
\tau_{rr}(r,\theta) &= -\frac{q_0E\alpha r^{-\frac{1}{2}}}{3\pi^2(1-\nu)}\cos\frac{\theta}{2}\left(1+\sin^2\frac{\theta}{2}\right)+O(r^0)\\
\tau_{rrn}(r,\theta) &= -\frac{3q_0E\alpha r^{-\frac{1}{2}}}{2\pi^2(1-\nu)}\cdot\frac{(-1)^n\cos k\theta'}{k^2-(\frac{3}{2})^2}\cos\frac{\theta}{2}\left(1+\sin^2\frac{\theta}{2}\right)+O(r^0)\\
\tau_{\theta\theta}(r,\theta) &= -\frac{q_0E\alpha r^{-\frac{1}{2}}}{3\pi^2(1-\nu)}\cos^3\frac{\theta}{2}+O(r^0)\\
\tau_{\theta\theta n}(r,\theta) &= -\frac{3q_0E\alpha r^{-\frac{1}{2}}}{2\pi^2(1-\nu)}\cdot\frac{(-1)^n\cos k\theta'}{k^2-(\frac{3}{2})^2}\cos^3\frac{\theta}{2}+O(r^0)
\end{aligned} \tag{A22}$$

$$\tau_{r\theta}(r,\theta) = -\frac{q_0 E\alpha r^{-\frac{1}{2}}}{6\pi^2(1-\nu)}\cdot\sin\theta\cos\frac{\theta}{2}+O(r^0)$$

$$\tau_{r\theta n}(r,\theta) = -\frac{3q_0 E\alpha r^{-\frac{1}{2}}}{4\pi^2(1-\nu)}\cdot\frac{(-1)^n\cos k\theta'}{k^2-(\frac{3}{2})^2}\sin\theta\cos\frac{\theta}{2}+O(r^0).$$

Thus, the convolution integrals, (A18), give the stresses as

$$\begin{aligned}
\sigma_{rr} &= -\frac{q_0 E\alpha}{6\pi^2(1-\nu)}\cos\frac{\theta}{2}\left(1+\sin^2\frac{\theta}{2}\right)r^{-\frac{1}{2}}r'^{-\frac{3}{2}}\tau+O(r^0)\\
\sigma_{\theta\theta} &= -\frac{q_0 E\alpha}{6\pi^2(1-\nu)}\cos^3\frac{\theta}{2}r^{-\frac{1}{2}}r'^{-\frac{3}{2}}\tau+O(r^0)\\
\sigma_{r\theta} &= -\frac{q_0 E\alpha}{12\pi^2(1-\nu)}\sin\theta\cos\frac{\theta}{2}r^{-\frac{1}{2}}r'^{-\frac{3}{2}}\tau+O(r^0)\\
\tau &= T\left(-\tfrac{1}{2},0,\frac{r'}{2\sqrt{(\kappa t)}}\right)+2\sum_{k=1}^{\infty}\frac{(-1)^k\cos k\theta'}{[1-(2k/3)^2]}T\left(k-\tfrac{1}{2},k,\frac{r'}{2\sqrt{(\kappa t)}}\right).
\end{aligned}\tag{A23}$$

The stress state established by equations (A18) or (A23) represents the fundamental solution for all boundary-value problems of a wedge. To examine the stresses resulting from other thermal distributions one need not resolve the stress problem subject to a new thermal environment. Rather, the stresses may be obtained directly from these results by considering them in the appropriate way.

For example, consider the case of heat emission from a source, stationary to the coordinate system (x, y), and past which the medium moves with constant velocity V in the direction of the positive x-axis. The corresponding stress state at time t and the location (x, y) due to the heat $q_0\,dt'$ emitted at t' is then by (A18) simply,

$$\sigma^*_{ij} = \int_0^t \sigma_{ij}[\{x-V(t-t')\}, y, (t-t')]\,dt'. \tag{A24}$$

For heat emission constant in time, as $t\to\infty$, a steady thermal régime is established in the medium and a quasi-static thermoelastic stress state, $\sigma^*_{ij}(x, y, V)$, results.

(*Received* 18 *January* 1968)

Абстракт—Исследуютсн эффекты возникновения тепла вследствие пластических деформаций, которые появляются на вершине движущейса трешины в квази-хрупких материалах. Рассматриваются изменения в окружающим поле упругих напряжений, для случая лолу-боесконечной, движущейся трешины, с иостоянной скоростью. Константируется, что напряжения, непосредственно предигествующие распространяющуюся трещину, уменьшаются, с точки зрения интенсивности, как естественное следствие необратимости материала. Величина этого уменьшения увеличивается с повышением скорости трещины